BASIN AND SUB-BASIN RESPONSE TO LONG-PERIOD GROUND MOTION: IMPLICATION FROM THE 3D FINITE-DIFFERENCE SIMULATION

Shin Aoi[1], Nobuyuki Morikawa[2] and Hiroyuki Fujiwara[3]

[1] *Senior Researcher, National Research Institute for Earth Science and Disaster Prevention, Tsukuba, Japan*
[2] *Researcher, National Research Institute for Earth Science and Disaster Prevention, Tsukuba, Japan*
[3] *Senior Researcher, National Research Institute for Earth Science and Disaster Prevention, Tsukuba, Japan*
Email: aoi@bosai.go.jp

ABSTRACT :

The 2003 Tokachi-oki earthquake (Mw 8.3) generated significant long-period ground motion and extended duration of a few hundred seconds in the Yufutsu basin, where oil tanks at Tomakomai were damaged by sloshing due to the long-period ground motion. General characteristics of long-period ground motion due to the combination of a large earthquake and a deep sedimentary basin were reproduced by large-scale finite-difference (FD) simulation in a period range of 3.3 to 25 s. In order to obtain a quantitative understanding of the long-period ground motion, we herein focus on the basin and sub-basin response on long-period ground motion in the Yufutsu basin. Visualization of the 3D FD simulations indicates that the surface waves from the source direction are amplified in both the eastern and western parts of the basin at the first 100 s. During the next 100 s, the surface waves are still trapped inside the sub-basin composed of shallow layers, and these layers amplified ground motions and extended the duration in the western part of the basin. A series of computations with/without each velocity layer in the basin revealed the basin response to be amplified 1.5 to 2 times, and the sub-basin response as an extension of ground motion durations and amplification was revealed to be approximately 1.5 times. Our 3D FD simulations quantitatively clarified that the combination of both the basin and sub-basin response is essential for understanding of disastrous long-period ground motions in the Yufutsu basin during the 2003 Tokachi-oki earthquake.

KEYWORDS: Long-period ground motion, 3D finite-difference simulation, 2003 Tokachi-oki earthquake, basin response, sub-basin response

1. INTRODUCTION

The 2003 Tokachi-oki, Japan, earthquake (Mw 8.3, depth = 42 km), which occurred along the Kuril trench, reminds us of the significance of long-period ground motions. Significant long-period (2 to 20 s) ground motions of extended duration were observed in the Yufutsu basin located more than 200 km from the epicenter, where oil tanks were damaged at Tomakomai due to sloshing associated with the ground motions [e.g., Koketsu et al., 2005]. A total of 655 K-NET and KiK-net stations [Kinoshita, 1998; Aoi et al., 2000, 2004] recorded ground motions during this event, and at the K-NET station in Tomakomai (HKD129), located in the western part of the Yufutsu basin, long-period ground motions (T > 5 s) continued for more than 200 s. Long-period ground motions in distant basins have been observed since the 1964 Niigata, Japan, earthquake [Kudo et al., 2000] and one of the most famous examples of an earthquake that excited long-period ground motions in a distant basin is the 1985 Michoacan, Mexico, earthquake [Anderson et al., 1986].
To obtain a quantitative understanding of the generation of long-period ground motions during the 2003 Tokachi-oki earthquake, we examined the basin and sub-basin responses of the Yufutsu basin in terms of exciting long-period ground motions using 3D finite-difference method (FDM).

2. OBSERVED LONG-PERIOD GROUND MOTIONS ALONG THE "YUFUTSU LINE"

We examined the generation and development of long-duration surface waves in velocity ground motions along the "Yufutsu line" from Cape Erimo to the Yufutsu basin (Fig. 1). The observed waveforms are shown by black

lines in Fig. 2. The stations located near the fault area (Group A) are situated upon rock, with just a thin layer of sediment or weathered rock. Consequently, the observed waveforms are simple. For the stations in Groups B and C, although the epicenter distances are larger, direct waves are more strongly amplified than those of Group A. In addition, the amplitude and durations are larger and longer than those of Group A because of the soft sediment within the Yufutsu basin. This effect is especially pronounced in the western part of the basin (Group C). For stations situated on rock on the far side of the basin (Group D), the waveforms are again simple, with small amplitudes.

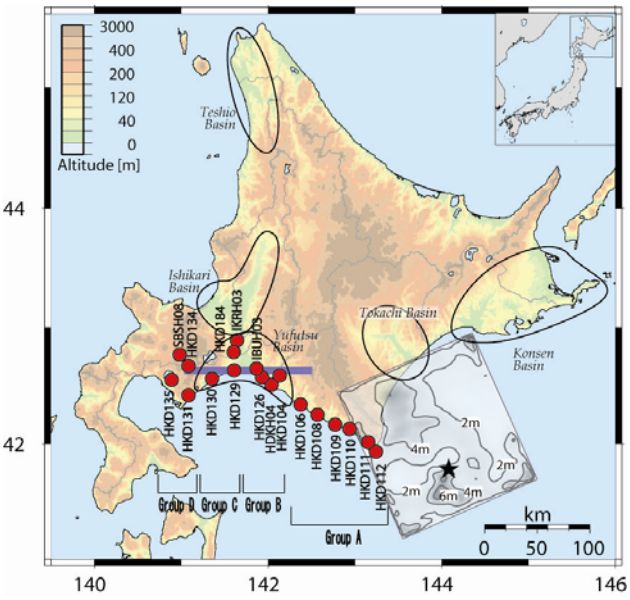

Figure 1 Locations of stations used in the present study and the fault model (distribution of total slip). The star indicates the hypocenter. The circles represent the stations of the Yufutsu line from Cape Erimo to the Yufutsu basin, which are used for the 3D FD simulation in comparing observed and simulated waveforms. These stations are classified into four groups. Group A: sites located upon rock; Group B: eastern part of the Yufutsu basin; Group C: western part of the Yufutsu basin; and Group D: sites located upon rock on the far side of the basin. The purple line indicates the location of the cross-sections of the 3D velocity structure models shown in Fig. 4.

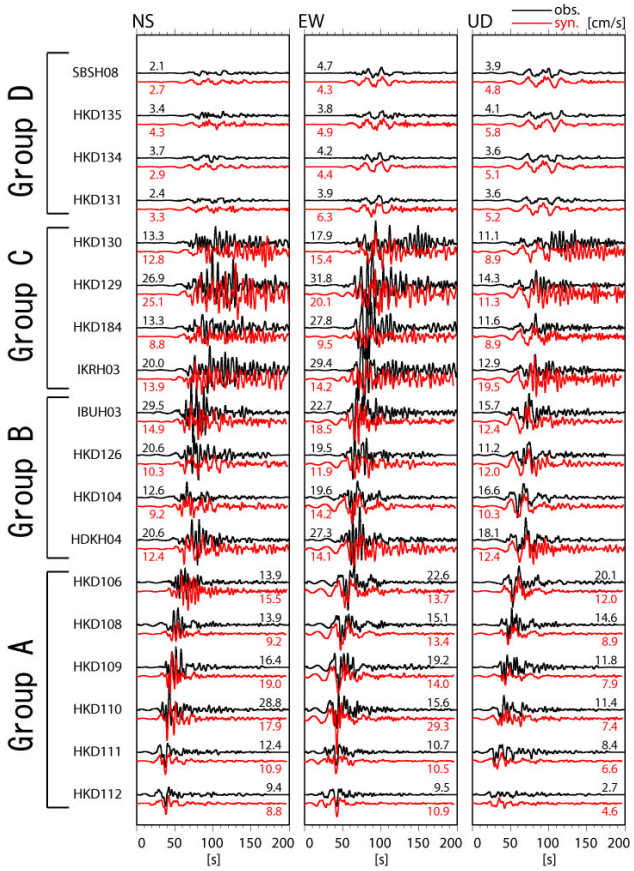

Figure 2 Comparison of observed (black lines) and synthetic (red lines) velocity waveforms for a period range of 3.3-25 s along the Yufutsu line. The locations of stations are indicated by the red circles in Fig. 1. Waveforms are plotted in the same scales for all components for all stations, and the numbers that accompany each trace show the maximum amplitude in cm/s.

3. SOURCE AND 3D VELOCITY STRUCTURE MODELS

We updated the source model of Honda et al. [2004] for the 2003 Tokachi-oki earthquake using the multi-time-window linear waveform inversion method [Hartzell and Heaton, 1983] with convolution of moving dislocation to represent the rupture propagation in each subfault [Sekiguchi et al., 2002]. Using K-NET and KiK-net data, Honda et al. [2004] deduced the rupture process of the earthquake by waveform inversion analysis for a period range of 5 to 50 s. Here, we update their rupture model to the extended period range of 2.5 to 50 s. The estimated total slip distribution is shown in figure 1.

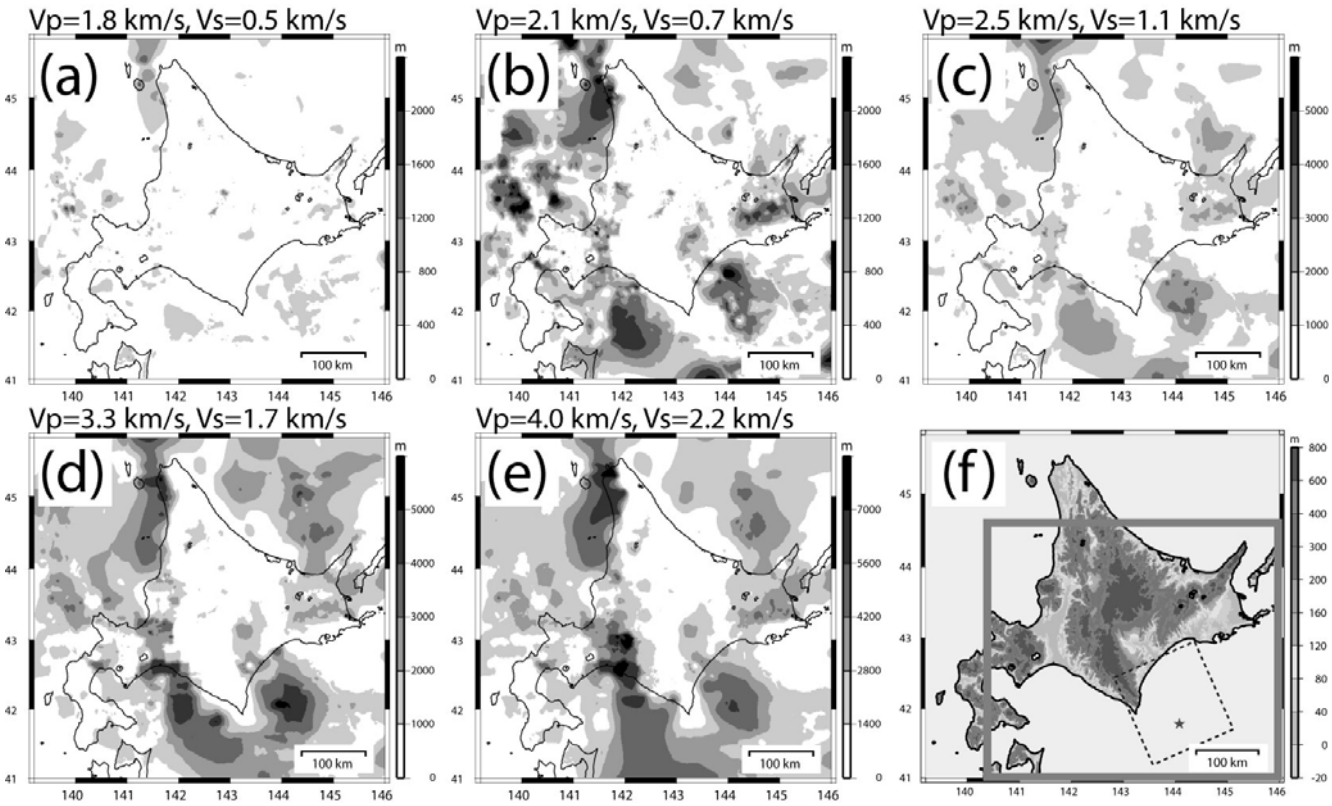

Figure 3 The 3D velocity structure model used above the 1D velocity and density profiles of the crust and upper mantle structure [Iwasaki et al., 1991] for the wider Hokkaido area. The figures show the depths of the lower surfaces of the (a) Quaternary, (b) Pliocene, (c) Late Miocene, (d) Middle Miocene, and (e) Early Miocene to Late Cretaceous. The depth shown in (e) corresponds to the depth to the basement. An elevation map of the area is shown in (f). The thick gray and dashed rectangles indicate the areas of the 3D FD simulation and the fault model, respectively. The star indicates the hypocenter.

Table 1 Physical parameters for sediment layers and basement rock that were used for the 3D FD simulation.

Layer No.	Vp [m/s]	Vs [m/s]	Density [kg/m^3]	Q	Geological Age
1	1800	500	1900	100	Quaternary
2	2100	700	2000	250	Pliocene
3	2500	1100	2200	1000	Late Miocene
4	3300	1700	2300	1000	Middle Miocene
5	4000	2200	2450	1000	Early Miocene - Late Cretaceous
6	Crust and upper mantle [*Iwasaki et al.*, 1991] 6000 < Vp < 8200, 3550 < Vs < 4630				Basement rock

We used the 1D structure model for the crust and upper mantle proposed by Iwasaki et al. [1991] with the 3D velocity structure model for sedimentary layers in order to model the observed complex patterns of wave propagation. The 3D velocity structure model with sedimentary layers for the Hokkaido region was modeled by compiling the results of reflection and refraction surveys, microtremor array observations, and deep borehole data of foundation drillings [Aoi et al., 2008]. Many on-land and offshore reflection surveys and deep borehole drillings have been undertaken within the Hokkaido region in the search for oil and gas. The 3D velocity structure model consists of five sedimentary layers above the seismic bedrock (Table 1), which is consistent with the stratigraphy of the target region. The seismic velocity of each layer is set to be uniform, and each layer

is assigned an average velocity as measured by VSP survey or sonic soundings. Figure 3 shows the distributions of the lower surfaces of the sedimentary layers employed in the 3D velocity structure model. The lower surface of the Vs = 2,200 m/s layer (Fig. 3e) corresponds to the depth to the basement. The deepest point of the top of the basement beneath the on-land areas lies within the Yufutsu basin. At this point, the base of the Vs = 1,100 m/s layer is located at a depth of approximately 3,800 m, and the base of the Vs = 2,200 m/s layer, corresponding to the depth to the basement, is approximately 8 km.

4. METHOD

We simulate long-period ground motions using a 3D FD simulation with discontinuous grids [Aoi and Fujiwara, 1999]. To accommodate details of 3D subsurface structures into the FD model, we employ the discontinuous grids that consist of a fine grid spacing of 250 m for regions shallower than 10 km that contain low-velocity sedimentary layers and a coarse grid spacing of 750 m for deeper regions. The use of discontinuous grids enabled us to reduce both the time and memory requirements of the computation to approximately 1/7 of that required when using a 250 m grid spacing for the entire region.
To investigate the generation and propagation of long-period ground motions, we examined the velocity waveforms of a linear array toward the Yufutsu basin, i.e. along the Yufutsu line. The stations are indicated by the red circles in Fig. 1. We attained good agreement between observed (black lines in Fig. 2) and synthetic (FDM; red lines in Fig. 2) velocity waveforms in the period range from 3.3 to 25 s, for areas both inside and outside the Yufutsu basin. We were also successful in reproducing later phases with large amplification and extended durations, as well as direct waves, at stations in the Yufutsu basin (Groups B and C). The degree of amplification and extended duration is remarkable in the western part of the Yufutsu basin (Group C), even though the basement is deeper and the sediment thicker in the eastern part. This apparent discrepancy can be explained by the fact that the waves are trapped in the shallow Quaternary, Pliocene, and Late Miocene layers with a Vs of less than 1,100 m/s, and these layers are considerably thicker in the western part of the basin. Waves are trapped in these soft sediment layers, and continue for several hundred seconds by propagating back and forth within the basin. We will discuss the mechanisms of this phenomenon in the next section. Our 3D FD simulation provides a quantitative explanation of the amplitudes, durations, and shape of the waveforms.

5. BASIN AND SUB-BASIN RESPONSES

The main feature of the long-period ground motions observed in the Yufutsu basin was that they were amplified in both the eastern and western parts of the basin, with much longer durations in the western part. Overall, the Yufutsu basin contains an internal sub-basin within the basin. The main basin deepens from west to east, reaching a maximum depth of more than 7 km. In contrast, the sub-basin deepens from east to west and has a maximum depth of 1 km or more (Fig. 4a). As stated in the previous section, the employed 3D velocity structure model consists of Layers 1, 2, 3, 4, 5, and 6, representing the Quaternary (Vs = 500 m/s), Pliocene (Vs = 700 m/s), Late Miocene (Vs = 1,100 m/s), Middle Miocene (Vs = 1,700 m/s), Early Miocene to Late Cretaceous (Vs = 2,200 m/s), and basement rock (Vs = 3,550 m/s or more depending on the depth modeled in Iwasaki et al. [1991]), respectively. The numbers of layers are introduced in Table 1. As a whole, the basin consists of Layers 1 to 5, while the sub-basin consists of Layers 1 to 3. In order to clarify the basin and sub-basin responses during the 2003 Tokachi-oki earthquake, we tested the following four models.

Model 123456 (Fig. 4a):
With all layers (basin with sub-basin + basement)
Model 444456 (Fig. 4b):
Without shallow layers in the basin (basin without sub-basin + basement)
Model 123666 (Fig. 4c):
Without deep layers in the basin (sub-basin + basement)
Model 666666 (Fig. 4d):
Without all layers (only basement)

Figure 5 compares the observed and synthetic ground velocities for the above four models using 3D FD simulations. Model 123456 is the same 3D velocity model as that used in the previous section, and the simulated velocity waveforms are in good agreement with the observed waveforms. Model 444456 was developed to assess the contribution of the deep sedimentary layers within the basin; in the model, the majority of the amplification is reproduced in the eastern part of the basin, with that in the western part being only approximately 50% of the observed values (Fig. 6). This model is unable to generate ground motions of extended duration. Model 123666 was developed to assess the contribution of the sub-basin. In this model, extended duration and only 50% of the observed amplification were reproduced in the western part of the basin. The underestimation of the degree of amplification produced by this model suggests that the sub-basin structure alone is insufficient in terms of explaining the generation mechanisms of long-period ground motion in the western part of the basin. Model 666666 is the case without any basins. This model failed to produce any amplification of ground motion or extended duration.

Figure 7 compares snapshots of the 3D simulation along the cross-section given by the purple line in Fig. 1. The snapshots reveal that the surface waves from the source direction are amplified throughout the entire basin during the first 100 s. In the following 100 s, the surface waves remain trapped inside the sub-basin (Layers 1 to 3), and these layers act to amplify the ground motions and prolong their duration in the western part of the basin. Our computation indicates that the basin effects result in an amplification of ground motions that are 1.5 to 2 times those outside the basin, and the sub-basin effects result in prolonged ground motion and an amplification that is 1.5 times that outside the basin (Fig. 6).

The importance of the interaction between the basin and sub-basin responses has been demonstrated qualitatively using 2D numerical simulations [e.g., Kawase and Aki, 1989; Graves, 1995; Hatayama et al. 2007]. Our 3D FD simulations provide quantitative evidence that a combination of the basin and sub-basin responses is essential in understanding the disastrous long-period ground motions that occurred in the Yufutsu basin during the 2003 Tokachi-oki earthquake.

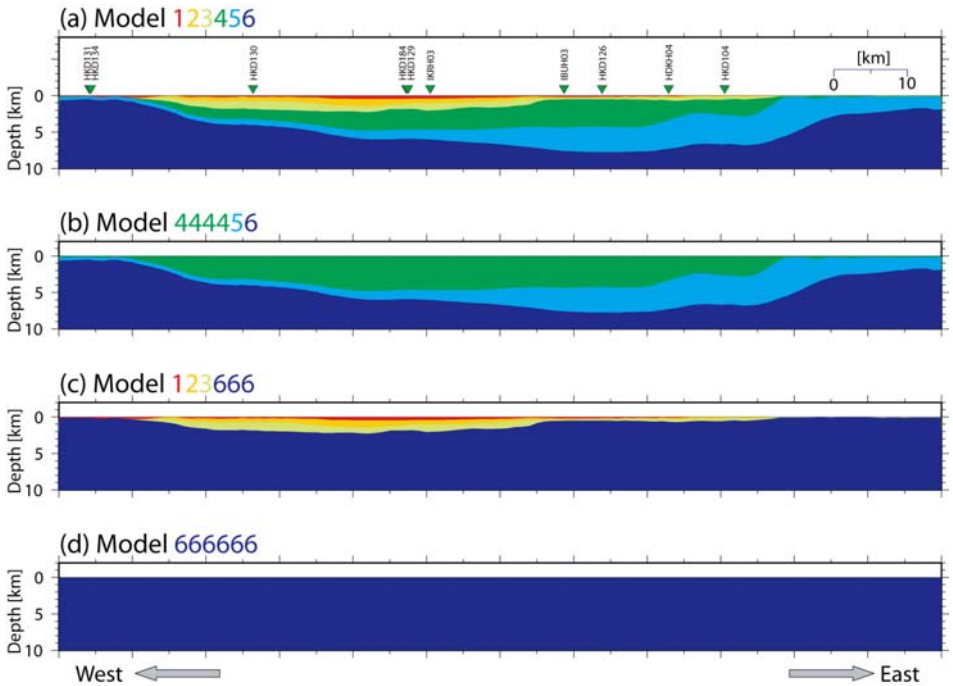

Figure 4 Cross-sections through the four employed 3D velocity structure models of the Yufutsu basin (sections are oriented along the purple line shown in Fig. 1). The model name is the combination of layer numbers in Table 1. (a) Model 123456: Full 3D velocity model for the Yufutsu basin, including the basin and sub-basin structures above the basement. (b) Model 444456: As for (a), but without the sub-basin structure. (c) Model 123666: As for (a), but without the main basin structure. (d) Model 666666: Velocity model composed solely of basement rock.

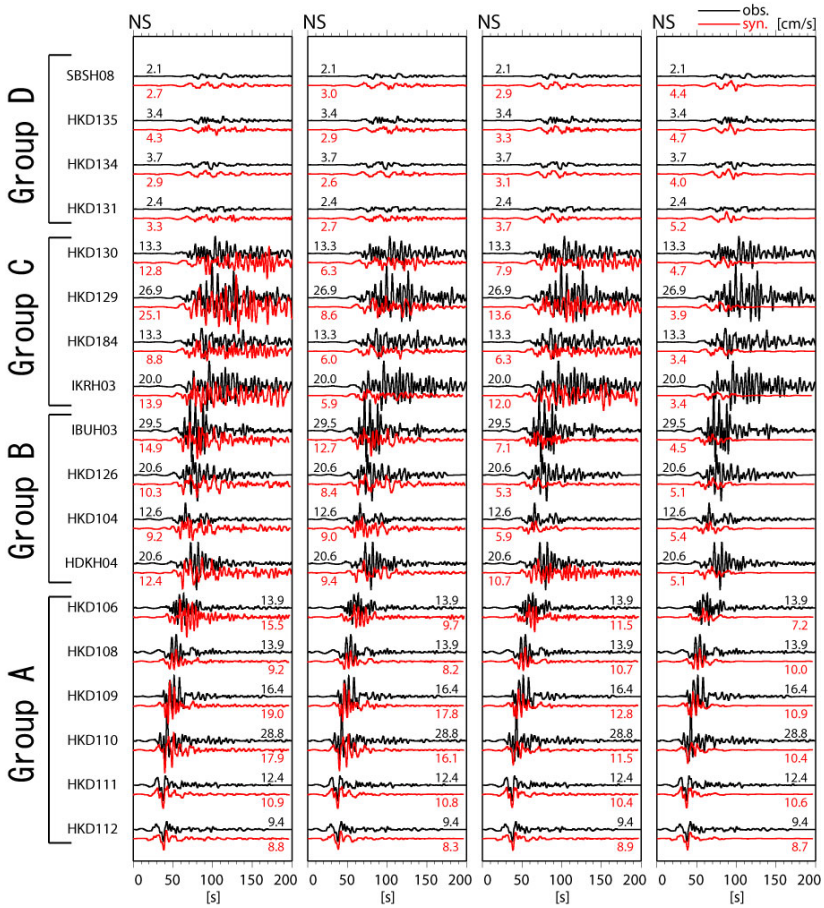

Figure 5 Results of a 3D FD simulation along the Yufutsu line designed to assess the basin and sub-basin responses. From left to right, the figures show the results obtained for Models 123456, 444456, 123666, and 666666, which compare the observed (black lines) and synthetic (red lines) velocity waveforms for a period range of 3.3-25 s. The locations of the stations are indicated by the red circles in Fig. 1. Waveforms are normalized by the maximum observed amplitude of each station, and the numbers that accompany each trace show the maximum amplitude in cm/s.

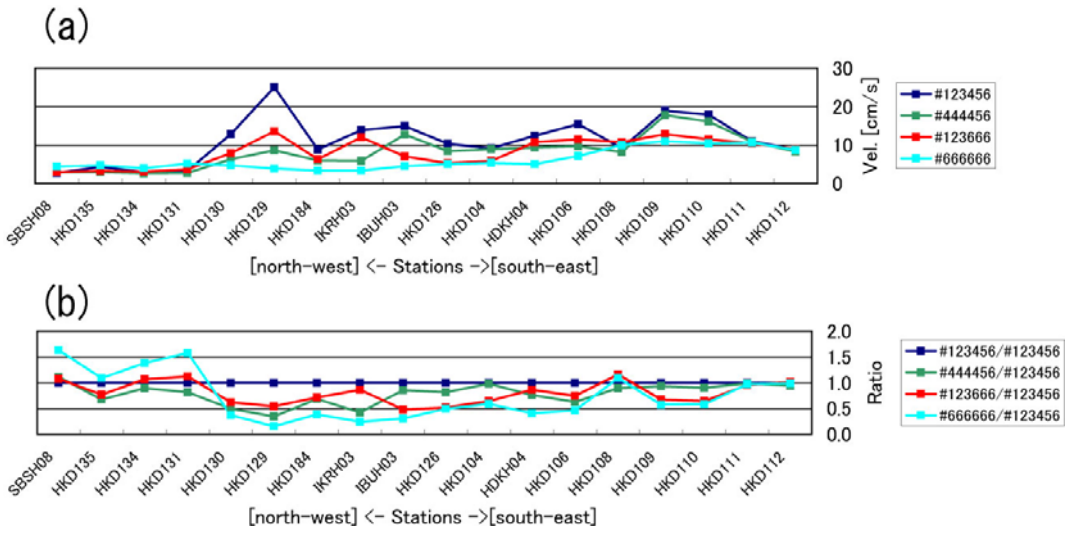

Figure 6 (a) Simulated PGVs (peak ground velocities) at each Yufutsu-line station for four models. (b) Ratios of simulated PGVs between model 123456 and each model.

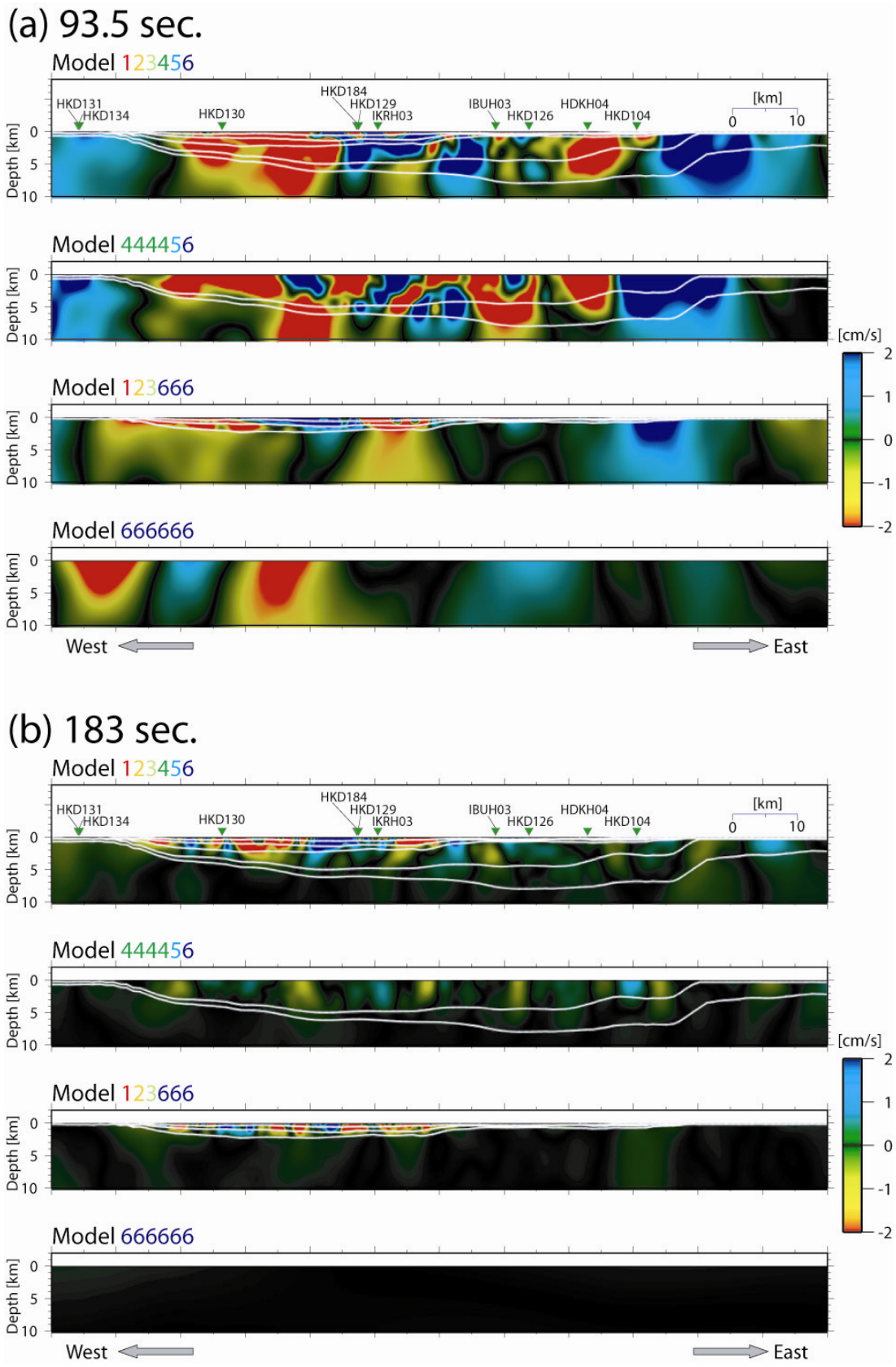

Figure 7 (a) Snapshots of vertical cross-sections of the wavefields for the four models simulated using FDM at 93.5 s. The cross-section location is given by the purple line in Fig. 1. From top to bottom, the figures show snapshots for Models 123456, 444456, 123666, and 666666. (b) Snapshot at 183 s.

6. CONCLUSION

The FD simulation successfully explained the development of amplified long-period ground motions of extended duration within the Yufutsu basin. The long-period ground motions were amplified in both the eastern and western parts of the basin, with their durations being strongly prolonged in the western part. A series of computations with/without each velocity layer in the basin clarified both the basin and sub-basin responses. The former amplifies long-period ground motions, while the latter amplifies and extends long-period ground motions. Our quantitative 3D FD simulations conclude that a combination of the basin and sub-basin responses generated the disastrous long-period ground motions that occurred within the Yufutsu basin during the 2003 Tokachi-oki earthquake.

ACKNOWLEDGEMENTS

This research was partly supported by a Grant-in-Aid for Scientific Research (A) (19201034).

REFERENCES

Anderson, J.G., Bodin, B., Brune, J.N., Prince, J., Singh, S.K., Quaas, R. and Onate, M. (1986). Strong ground motion from the Michoacan, Mexico, earthquake. *Science*, **233**, 1043-1049.

Aoi, S., Obara, K., Hori, S., Kasahara, K. and Okada, Y. (2000). New strong-motion observation network: KiK-net. *EOS. Trans. AGU*, **81(48)**, Fall Meet. Suppl., Abstract S71A-05.

Aoi, S. and Fujiwara. H. (1999). 3D finite-difference method using discontinuous grids. *Bull. Seismol. Soc. Am.*, **89**, 918-930.

Aoi, S., Kunugi, T. and Fujiwara, H. (2004). Strong-motion seismograph network operated by NIED: K-NET and KiK-net. *J. Japan Assoc. Earthq. Eng.*, **4**, 65-74.

Aoi, S., Honda, R., Morikawa, N., Sekiguchi, H., Suzuki, H., Hayakawa, Y., Kunugi, T. and Fujiwara, H. (2008). Three-dimensional finite difference simulation of long-period ground motions for the 2003 Tokachi-oki, Japan earthquake. *J. Geophys. Res.*, **113**, B07302, doi:10.1029/2007JB005452.

Graves, R.W. (1995). Preliminary analysis of long-period basin response in the Los Angeles region from the 1994 Northridge earthquake. *Geophys. Res. Lett.* **22**, 101-104.

Hartzell, S.H. and Heaton, T.H. (1983). Inversion of strong ground motion and teleseismic waveform data for the fault rupture history of the 1979 Imperial Valley, California, earthquake. *Bull. Seism. Soc. Am.*, **73**, 1553-1583.

Hatayama, K., Kanno, T. and Kudo, K. (2007). Control factors of spatial variation of long-period strong ground motions in the Yufutsu sedimentary basin, Hokkaido, during the Mw 8.0 2003 Tokachi-oki, Japan, earthquake. *Bull. Seismol. Soc. Am.*, **97**, 1308-1323.

Honda, R., Aoi, S., Morikawa, N., Sekiguchi, H., Kunugi, T. and Fujiwara, H. (2004). Ground motion and rupture process of the 2003 Tokachi-oki earthquake obtained from strong motion data of K-NET and KiK-net. *Earth Planets Space*, **56**, 317-322.

Iwasaki, T., Hirata, N., Kanazawa, T., Urabe, T., Motoya, Y. and Shimamura, H. (1991). Earthquake distribution in the subduction zone off eastern Hokkaido, Japan, deduced from ocean-bottom seismographic and land observations. *Geophys. J. Int.*, **105**, 693-711.

Kinoshita, S. (1998). Kyoshin net (K-NET). *Seismol. Res. Lett.*, **69**, 309-332.

Kawase, H. and Aki, K. (1989). A study on the response of a soft basin for incident S, P, and Rayleigh waves with special reference to the long duration observed in Mexico City. *Bull. Seismol. Soc. Am.*, **79**, 1361-1382.

Koketsu, K., Hatayama, K., Furumura, T., Ikegami, Y. and Akiyama, S. (2005). Damaging long-period ground motions from the 2003 Mw 8.3 Tokachioki, Japan, earthquake. *Seismol. Res. Lett.*, **76**, 67-73.

Kudo, K., Uetake., T. and Kanno, T. (2000). Re-evaluation of nonlinear site response during the 1964 Niigata earthquake using the strong motion records at Kawagishi-cho, Niigata City. *Proc 12th World Conf. Earthq. Eng.*, No. 0969.

Sekiguchi, H., Irikura, K. and Iwata, T. (2002). Source inversion for estimating continuous slip distribution on the fault, -Introduction of Green's functions convolved with a correction function to give moving dislocation effects in subfaults-. *Geophys. J. Int.*, **150**, 377-391.